

Comparing the paleoclimates of northwestern and southwestern Madagascar during the late Holocene: Implications for the role of climate in megafaunal extinction

Peterson Faina¹, Stephen J. Burns², Laurie R. Godfrey³, Brooke E. Crowley^{4,5}, Nick Scroxton⁶, David McGee⁷, Michael R. Sutherland⁸ & Lovasoa Ranivoarimanana¹

¹ Bassins sédimentaires Evolution Conservation, Faculté des Sciences, Université d'Antananarivo, BP 906, Antananarivo 101, Madagascar
E-mail: petersonfaina@gmail.com, ranivolova@gmail.com

² Department of Geosciences, 611 North Pleasant Street, University of Massachusetts, Amherst, Massachusetts 01003, USA
E-mail: sburns@umass.edu

³ Department of Anthropology, 240 Hicks Way, University of Massachusetts, Amherst, Massachusetts 01003, USA
E-mail: lgodfrey@umass.edu

⁴ Department of Geology, University of Cincinnati, Cincinnati, Ohio 45221, USA

⁵ Department of Anthropology, University of Cincinnati, Cincinnati, Ohio 45221, USA
E-mail: brooke.crowley@uc.edu

⁶ Department of Geography, Maynooth University, Ireland

E-mail: nick.scroxton@mu.ie

⁷ Earth, Atmospheric and Planetary Sciences, Massachusetts Institute of Technology, 77 Massachusetts Avenue, Cambridge, Massachusetts 02139, USA
E-mail: davidmcg@mit.edu

⁸ Department of Mathematics and Statistics, University of Massachusetts, Amherst, Massachusetts 01003, USA
E-mail: mikes@math.umass.edu

Abstract

The relative importance of climate and humans in the disappearance of the Malagasy megafauna remains under debate. Data from southwestern Madagascar imply aridification contributed substantially to the late Holocene decline of the megafauna (the Aridification Hypothesis). Evidence for aridification includes carbon isotopes from tree rings, lacustrine charcoal concentrations and pollen assemblages, and changes in fossil vertebrate assemblages indicative of a local loss of pluvial conditions. In contrast, speleothem records from northwestern Madagascar

suggest that megafaunal decline and habitat change resulted primarily from human activity including agropastoralism (the Subsistence Shift Hypothesis). Could there have been contrasting mechanisms of decline in different parts of Madagascar? Or are we lacking the precisely dated, high resolution records needed to fully understand the complex processes behind megafaunal decline?

Reconciling these contrasting hypotheses requires additional climate records from southwestern Madagascar. We recovered a stalagmite (AF2) from Asafora Cave in the spiny thicket ecoregion, ~10 km from the southwest coast and just southeast of the Velondriake Marine Reserve. U-series and ¹⁴C dating of samples taken from the core of this stalagmite provide a highly precise chronology of the changes in hydroclimate and vegetation in this region over the past 3000 years. Speleothem stable oxygen and carbon isotope analyses provide insight into past rainfall variability and vegetation changes respectively. We compare these records with those for a stalagmite (AB2) from Anjohibe Cave in northwestern Madagascar. Lastly, odds ratio analyses of radiocarbon dates for extinct and extant subfossils allow us to describe and compare the temporal trajectories of megafaunal decline in the southwest and the northwest. Combined, these analyses allow us to test the Aridification Hypothesis for megafaunal extinction.

The trajectories of megafaunal decline differed in northwestern and southwestern Madagascar. In the southwest, unlike the northwest, there is no evidence of decoupling of speleothem stable carbon and oxygen isotopes. Instead, habitat changes in the southwest were largely related to variation in hydroclimate (including a prolonged drought). The megafaunal collapse here occurred in tandem with the drought, and agropastoralism likely contributed to that demise only after the megafauna had already suffered drought-related population reduction. Our results offer some support for the Aridification Hypothesis, but with three caveats: first, that there was no island-wide aridification; second, that aridification likely impacted megafaunal decline only in the driest parts of Madagascar; and third, that aridification was not the sole factor promoting

megafaunal decline even in the dry southwest. A number of megafaunal species survived the prolonged drought of the first millennium, and then likely succumbed to the activities of agropastoralists.

Key words: subfossils, stalagmites, stable carbon isotopes, stable oxygen isotopes, climate change, subsistence shift hypothesis, ^{14}C and $^{230}\text{Th}/\text{U}$ age determinations

Résumé détaillé

L'importance relative du climat et de l'homme dans la disparition des mégafaunes de Madagascar fait l'objet d'un débat continu. Les données du Sud-ouest de Madagascar impliquent que l'aridification a contribué de manière substantielle au déclin des mégafaunes à la fin de l'Holocène (hypothèse de l'aridification). Parmi les preuves de l'aridification comprennent les isotopes de carbone des anneaux de croissance des arbres, les concentrations de charbon lacustre et les assemblages de pollen, ainsi que les preuves de la disparition des vertébrés fossiles indiquant une perte locale des conditions pluviales. Par contre, les enregistrements des spéléothèmes du Nord-ouest de Madagascar suggèrent que le déclin des mégafaunes et la modification de l'habitat résultent principalement de l'activité humaine, y compris l'agropastoralisme (Hypothèse de Changement de Subsistance). Aurait-il pu y avoir des mécanismes de déclin contrastés dans différentes parties de Madagascar ? Ou bien manquons-nous de données datées avec précision et à haute résolution, nécessaires pour comprendre pleinement les processus complexes qui soutiennent le déclin des mégafaunes ?

La conciliation de ces hypothèses contrastées nécessite des enregistrements climatiques supplémentaires dans le Sud-ouest de Madagascar. Une stalagmite (AF2) de la grotte d'Asafora dans l'écorégion des fourrés épineux, au Sud-ouest de Madagascar, à environ 10 km de la côte ouest et juste au sud-est de la réserve marine de Velondriake a été prélevée. Les datations U-Th et ^{14}C des échantillons prélevés sur cette stalagmite fournissent une chronologie très précise des changements de l'hydroclimat et de la végétation dans cette région au cours des 3000 dernières années. Les analyses des isotopes stables de l'oxygène et du carbone du spéléothème donnent un aperçu de la variabilité des précipitations du passé et des changements de la végétation respectivement. Nous comparons ces données avec celles d'une stalagmite (AB2) de la grotte d'Anjohibe, dans le Nord-ouest de

Madagascar. Enfin, les analyses de rapports de cotés des subfossiles éteints et existants datées par la datation au radiocarbone ont permis de décrire et de comparer les trajectoires du déclin des mégafaunes dans le Sud-ouest et le Nord-ouest. Combinées, ces analyses nous ont aussi permis de tester l'Hypothèse d'Aridification dans l'extinction de la mégafaune.

Les trajectoires de déclin des mégafaunes sont différentes dans le Nord-ouest et le Sud-ouest de Madagascar. De plus, dans le Sud-ouest, contrairement au Nord-ouest, il n'y a pas de preuve de découplage des isotopes stables du carbone et de l'oxygène du spéléothème. Au lieu de cela, les changements d'habitat dans le Sud-ouest ont été largement liés à la variation de l'hydroclimat (y compris une sécheresse prolongée). L'effondrement des mégafaunes ici s'est produit en même temps que la sécheresse, et l'agropastoralisme n'a probablement contribué à cette disparition qu'après que les mégafaunes aient déjà subis une réduction de population liée à la sécheresse. Les résultats offrent un certain soutien à l'Hypothèse de l'Aridification, mais avec trois mises en réserve : premièrement, qu'il n'y a pas eu d'aridification à l'échelle de l'île ; deuxièmement, que l'aridification a eu un impact sur le déclin des mégafaunes uniquement dans les parties les plus sèches de Madagascar ; et troisièmement, que l'aridification n'a pas été le seul facteur favorisant le déclin des mégafaunes, même dans le Sud-ouest aride. Un certain nombre d'espèces de mégafaunes ont survécu à la sécheresse prolongée du premier millénaire, puis ont probablement succombé aux activités des agropasteurs.

Mots clés : Subfossiles, stalagmites, isotopes stables de carbone, isotopes stables de l'oxygène, changement du climat, hypothèse de changement de subsistance, détermination des âges par ^{14}C et $^{230}\text{Th}/\text{U}$

Introduction

Madagascar today experiences a tremendous amount of climate variation from its northern to southern ends. The island is influenced by two seasons: the hot, rainy season (with tropical monsoons) from November to April, and the cool, dry season from May to October (Griffiths & Ranaivoson, 1972; Donque, 1975). Seasonal movement of the tropical rain belt (the Intertropical Convergence Zone, or ITCZ) results in the northwest receiving considerably more rainfall than the southwest (Vallet-Coulomb et al., 2006).

Madagascar is divided into five major ecoregions: humid forest, Central Highlands, dry deciduous forest, succulent woodland, and spiny thicket (Burgess et al., 2004). Each of these ecoregions is characterized by its own unique fauna and flora, but many taxa, at least at the genus level, exist across ecoregions. It is well known that Madagascar is one of the most threatened biodiversity hotspots on Earth (Goodman & Benstead, 2005) and its biodiversity was even greater in the recent past. Following human colonization more than 2000 years ago, the island experienced megafaunal extinctions and widespread deforestation, leaving many elements of modern ecosystems in a state of ecological disruption (Burney et al., 2004; Crowley, 2010). The peak of the collapse occurred around 1100 years before present (BP); by around 900 BP, megafauna were rare across the island (Godfrey et al., 2019). Records of megafauna are preserved at subfossil sites across much of Madagascar, and these now-extinct animals undoubtedly also once lived in places where no subfossil sites are known. As with extant taxa, there was regional endemicity of megafaunal species, but many of the genera were widespread. The paleontological record indicates that megafaunal populations collapsed during the late first millennium apparently simultaneously, despite the fact that these animals may have been experiencing very different climatic conditions across the diverse ecoregions in which they lived.

The relative impacts of human activities and climate change on extinction dynamics in Madagascar remains a subject of continued debate, with important contributions from specialists in diverse fields (such as paleontology, archaeology, and paleoclimatology) (Burney et al., 2004; Virah-Sawmy et al., 2010; Dewar et al., 2013; Burns et al., 2016; Virah-Sawmy 2016; Crowley et al., 2017; Godfrey et al., 2019). Given the fact that different regions of Madagascar have very different climates, it is unlikely that a simple change in rainfall would have affected all regions equally. Nevertheless, when the impact of climate change on megafaunal extinction is considered, the island has often been treated as a single entity with uniform fluctuations in precipitation. For example, some researchers have proposed that an island-wide mega-drought contributed to the disappearance of Madagascar's large vertebrates around 1000 years ago (Virah-Sawmy et al., 2010). While it is true that there was a significant megafaunal population decline across the island at that time, speleothem records from the northwest suggest that this region

was relatively wet when the local populations crashed (Godfrey et al., 2019). In contrast, southwestern paleoecological records (tree-ring carbon isotopes, lacustrine charcoal concentrations, and pollen assemblages) have suggested that aridification may have contributed to the decline of certain species in this region (Burney, 1993; Virah-Sawmy et al., 2016; Razanatsoa, 2019).

The timing of initial human colonization of Madagascar, as well as the role of humans in the extinction of Madagascar's megafauna, also remains a topic of intense debate. Evidence of human presence on the island exists in several forms. In addition to direct evidence of human cultural remains (Wright et al., 1996; Dewar et al., 2013; Douglass et al., 2018), researchers derive inferences indirectly from paleoecology (Burney, 1993; Burney et al., 2003, 2004; Virah-Sawmy et al., 2010), linguistics (Blench, 2010; Beaujard, 2019), genetics (Pierron et al., 2017), isotope values for animal bones (Crowley & Samonds, 2013), and speleothem isotope values (Burns et al., 2016; Railsback et al., 2020). More indirect evidence of human presence comes from traces of butchering of wild animals by humans on subfossil bones at paleontological sites (Pérez et al., 2005; Gommery et al., 2011; Hansford et al., 2018; Godfrey et al., unpublished data) and the introductions of domesticated plants and animals (Crowther et al., 2016; Sauther et al., 2020). In a review and evaluation of the quality of all of these data, Douglass et al. (2019) concluded that humans had arrived on Madagascar by at least 2000 years ago.

Different authors have supported alternative hypotheses regarding the triggers for megafaunal extinction, depending only in part on their interpretation of human colonization. These include Virah-Sawmy et al.'s (2010) island-wide Aridification Hypothesis, Burney et al.'s (2004) Synergy Hypothesis, Godfrey et al.'s (2019) Subsistence Shift Hypothesis, and others. In one of the earliest arguments in favor of aridification as the main trigger of megafaunal extinction, Mahé and Sourdat (1972) presumed that the megafauna suffered population reduction and local extirpations due to prolonged aridification long before humans arrived in southwestern Madagascar. Rejecting any major impact from human habitat modification or hunting pressure while acknowledging some (though they believed limited) temporal overlap for humans and megafauna, they concluded that megafaunal extinction began 3000 years ago in southwestern Madagascar, with waves

at 2200 and 1200 yr BP (Mahé & Sourdant, 1972). The disappearance of freshwater birds, coupled with evidence for salinization of previously freshwater lakes and a reduction in the number of coastal lakes and marshes, compelled Goodman and Rakotozafy (1997) to also support aridification as a significant trigger for extinction. These authors embraced the notion, earlier proposed by Mahé and Sourdant (1972), that the southwest had undergone an extended period of drying beginning ~3000 years ago. Virah-Sawmy *et al.* (2010) made the Aridification Hypothesis more explicit. They suggested that, at around 950 BP, the vegetation changed abruptly across the island, and that this occurred both in the presence and in the absence of sudden fire peaks, and thus could not be linked solely to human intervention. Instead, they argued that across Madagascar, ecosystems were impacted by climatic desiccation, which was the main trigger for megafaunal extinction.

The Aridification Hypothesis has been rejected by several authors. Crowley *et al.* (2017) used nitrogen isotope ($\delta^{15}\text{N}$) values from subfossil bones to study temporal variation in habitat moisture. They tested the Aridification Hypothesis across several ecoregions, including the spiny thicket, succulent woodland, dry deciduous forest, and Central Highlands, and rejected it because of the lack of a consistent, island-wide signal. They found evidence for site aridification only at Andolonomby (=Ambolisatra, $23^{\circ}3'28.20''\text{S}$, $43^{\circ}35'27.30''\text{E}$), a western coastal subfossil site 80 km south of Asafora Cave and 40 km north of Toliara (Figure 1). Hixon *et al.* (2018) drew conclusions similar to those of Crowley *et al.* (2017), based on a more refined study of the stable nitrogen isotopes of specific amino-acids for one extinct lemur, *Pachylemur*, and one extant lemur, *Propithecus*, at two inland subfossil sites in southwestern Madagascar: Tsirave (in the succulent woodland) and Taolambiby (in the spiny thicket). There was no evidence that either species experienced water stress or changed its diet. *Pachylemur* had consistent $\delta^{15}\text{N}$ values between ~3800 yr BP and ~900 yr BP when it finally disappeared at Tsirave. Similarly, Burns *et al.* (2016) and Scroxton *et al.* (2017) found no evidence of aridification in northwestern Madagascar over the past 2000 years. Instead, strong evidence of abrupt habitat transformation via deliberate burning in the northwest was unrelated to any change in rainfall amount.

The Synergy Hypothesis was developed by Burney (1999) and Burney *et al.* (2003, 2004). While these authors believed that climate change

and human activities acted synergistically to trigger megafaunal decline, they also considered human hunting to be primary among them. Spores of the dung fungus *Sporormiella* were taken as proxies for megaherbivore abundance, as this fungus can only reproduce on large feces. Burney *et al.* (2003) found similar sequences of events in sediment cores taken from southwestern (subarid), northwestern (dry), and Central Highland (subhumid) sites. Early in the first millennium CE, the *Sporormiella* spore counts were high; this was followed by a decrease in *Sporormiella* spores, and finally a spike in microscopic charcoal particles. This sequence of events was interpreted to signal that early and abundant megaherbivore populations were reduced through anthropogenic actions, particularly hunting, and that habitat transformation through natural as well as anthropogenic fires ensued, sparked by an increase in the biomass of grasses formerly controlled by the megaherbivores.

More recently, Godfrey *et al.* (2019) proposed the Subsistence Shift Hypothesis, which held that megafaunal population collapse was triggered not by early human arrival, but by a shift in subsistence from hunting and foraging to herding and farming, in turn associated with the expansion of the Indian Ocean trade network, the introduction of domesticated plants and animals, and an increase in human population size – all happening in the last several centuries of the first millennium CE. On the basis of a growing literature on wild-animal hunting in hunter-forager versus herder/farmer societies (Alvard, 1993; Robinson & Bennett, 2000; Winterhalder, 2001; Koch & Barnosky, 2006), Godfrey *et al.* (2019) proposed that hunting pressure on wild animals probably increased at this time. This is despite the increased availability of alternative food resources associated with the introduction of domesticated plants and animals. Certainly, there was also an increase in habitat modification through deliberate burning (Godfrey *et al.*, 2019).

Disentangling the effects of climate and human activities is often difficult because humans and climate can cause similar modifications of habitats. However, it is possible to disentangle these effects by measuring carbon ($\delta^{13}\text{C}$) and oxygen ($\delta^{18}\text{O}$) stable isotope values in speleothems such as stalagmites. These two isotopes are frequently used as proxies for vegetation cover and precipitation amount, respectively (Dorale *et al.*, 1998; McDermott, 2004; Fairchild, 2006; Wong & Breecker, 2015). Higher $\delta^{13}\text{C}$ values generally indicate increasingly open

vegetation cover and, in some cases, a shift to greater predominance of C₄ grasses. Speleothem δ¹⁸O values record changes in precipitation δ¹⁸O, which, in the tropics, are often inversely proportional to the amount of rainfall particularly in coastal (or near-coastal) areas (Lachniet, 2009). Speleothem δ¹⁸O and δ¹³C values are frequently correlated because of the effects of changing rainfall on vegetation cover and soil respiration rates, which in turn influence speleothem δ¹³C, and/or because of in-cave signal modification due to disequilibrium fractionation, itself likely forced by climate. The breaking of this relationship is therefore often interpreted as resulting from changes in δ¹³C forced by either non-linear vegetation responses to climate, or non-climatic land-use changes by humans, wildfires, volcanic eruptions, etc. (Scroxton, 2014; Akers et al., 2016; Burns et al., 2016). By measuring both isotopes through time, we can determine whether or not

habitat and total rainfall amount changed in tandem, or conversely, if the habitat changed without any modification in rainfall. When coupled with ²³⁰Th/U age determinations, speleothem stable isotope measurements provide information on the timing of changes in rainfall and vegetation that are often higher resolution and more precisely dated than many other paleoclimate proxies. The co-location of rainfall (δ¹⁸O) and vegetation (δ¹³C) proxies in the same climatic archive also allows for determination of the timing of rainfall and vegetation changes. Together, this precision helps to separate the effects of humans versus climate on regional vegetation change. Over the past decade, several studies of stalagmite records from northwestern Madagascar have helped to elucidate the paleoclimate and vegetation history of this region during the late Holocene (Burns et al., 2016; Scroxton et al., 2017; Voarintsoa et al., 2017; Wang et al., 2019; Railsback et al., 2020). However,

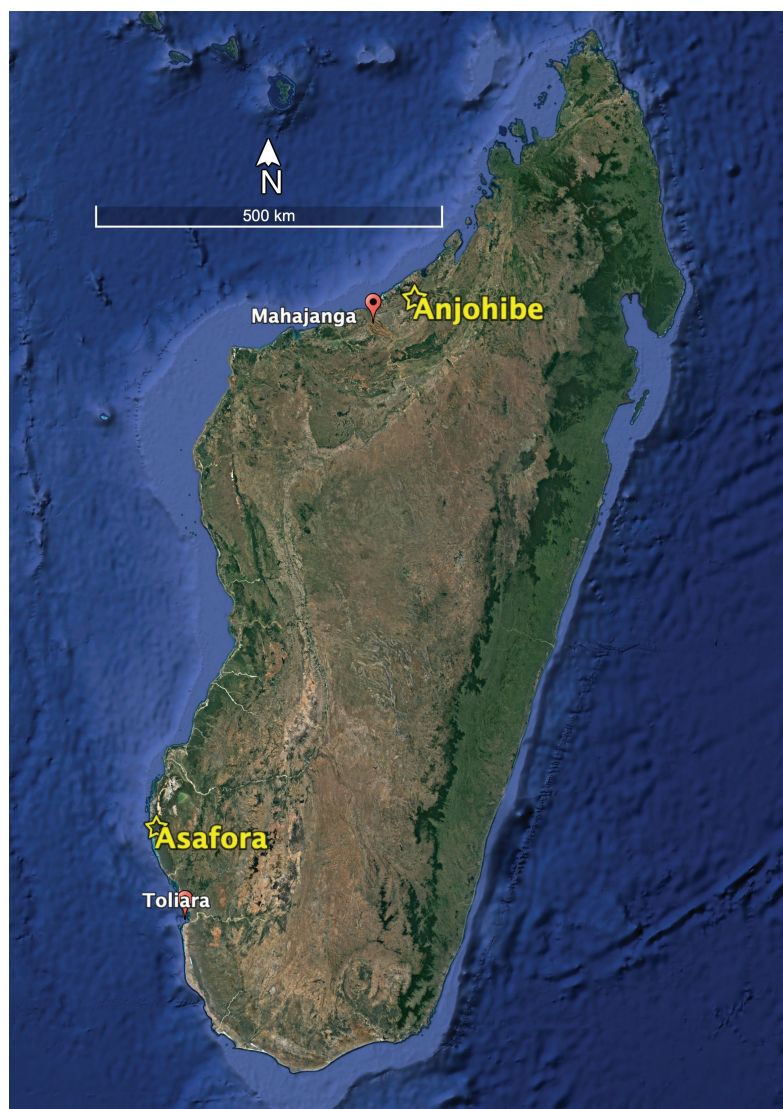


Figure 1. Map showing locations of Anjohibe (dry deciduous forest) and Asafora (dry spiny thicket) Caves, with nearest major cities.

until now, there have been no speleothem records of climate change during the late Holocene in the southwest.

A recent study (Scroxton et al., 2019) of a speleothem from southwestern Madagascar that covered the Late Pleistocene including the last deglaciation period (21–11.6 kyr BP) showed that changes in the regional climate were complex and influenced by a variety of factors including both shifts in the ITCZ and changes in sea surface temperature. It follows that we cannot expect that parallel climate changes would have occurred in the north (typically interpreted as resulting from changes in the tropical rain belt) and southwest when the megafaunal populations crashed.

This article provides a new detailed climate record for southwestern Madagascar during the late Holocene based on a stalagmite (AF2) collected at Asafora Cave, which is located ~120 km north of Toliara (Figure 1). We use these records to test the hypothesis that the southwest experienced a megadrought event when the megafaunal populations in that region crashed. We then compare the AF2 speleothem data to prior records from the northwest (AB2 from Anjohibe) to test the hypothesis that parallel climate fluctuations occurred in these two regions. Next, we use radiocarbon records of megafauna from the northwest and the southwest to determine when their populations collapsed and if they did so simultaneously. Lastly, we ask how this work informs our understanding of the roles of

climate and other factors (such as a human activity) in megafaunal extinction across Madagascar.

Material and methods

Speleothem sampling and the construction of an age model

Stalagmite AF2 was collected in 2015 at Asafora Cave ($22^{\circ}19'10.92''S$, $43^{\circ}19'21.06''E$), just southeast of Murder Bay (Baie des Assassins) and the Velondriake Marine Reserve in the district of Morombe, southwest Madagascar. This region today experiences an average annual temperature of 24.4°C and mean annual precipitation of ~460 mm (<https://en.climate-data.org/africa/madagascar/andavadoaka/andavadoaka-635546/>, accessed 6/30/2020). The regional vegetation is dry spiny thicket (Goodman et al., 2018); it is dominated by both trees and shrubs adapted to a dry climate. C_3 plants include *Adansonia*, *Commiphora*, *Dalbergia*, and *Tamarindus*, while CAM plants include *Didierea* and *Euphorbia*. Ground cover is sparse and consists of a mix of herbaceous vegetation and C_4 grasses.

The stalagmite was vertically sliced, polished and microdrilled along the central growth axis at the University of Massachusetts Amherst, Department of Geosciences Stable Isotope Laboratory (Figure 2). We collected 770 subsamples from AF2 perpendicular to growth layers (one every 0.2 mm, i.e., approximately one every 4 years). Subsamples from AF2 were prepared using a Thermo Scientific Gas Bench II for analysis on a Thermo Delta V



Figure 2. Cut and polished slab of stalagmite AF2 from Asafora Cave showing internal layering.

Table 1. ^{14}C age data for stalagmite AF2 (Asafora Cave) calibrated ages.

z (distance in mm from top)	^{14}C Age	$\pm 1\sigma$	Calibrated Age (Cal yr BP)				
			Min	Max	Median	Mean	$\pm 1\sigma$
4	>Modern	140				0	
28	780	140	510	925	692	717.5	207.5
44	890	140	550	985	782	767.5	217.5
58	1150	140	760	1285	1024	1022.5	262.5
70	1440	150	1045	1580	1303	1312.5	267.5
97	2110	140	1715	2350	2051	2032.5	317.5
104	2030	140	1690	2315	1953	2002.5	312.5
115	2980	160	2755	3450	3099	3102.5	347.5
128	2660	160	2335	3080	2702	2707.5	372.5
134	3150	160	2875	3645	3295	3260	385

Advantage mass spectrometer. Resulting $\delta^{13}\text{C}$ and $\delta^{18}\text{O}$ values are recorded as per thousand (‰) relative to the Vienna PeeDee Belemnite (VPDB) standard.

Ten AMS ^{14}C and two $^{230}\text{Th}/\text{U}$ age determinations were made on subsamples of AF2 (Tables 1 & 2). For ^{14}C age determinations, approximately 30 mg chips of solid calcite were cut from the growth axis of one half of the stalagmite. The samples were analyzed by Gas Ion Source methodology (sample numbers OS-150680 to OS-150689) at the National Ocean Sciences Accelerator Mass Spectrometry facility at the Woods Hole Oceanographic Institute. Radiocarbon ages (^{14}C yr before present) were converted to calendar years before present using the SHCal13 calibration curve in Calib 7.1 (Hogg et al., 2013; Stuiver et al., 2020). We present average calibrated dates ± 1 standard deviation (1σ) based on 2σ ranges (Table 1). The two $^{230}\text{Th}/\text{U}$ age determinations were analyzed at the Massachusetts Institute of Technology. Samples weighing 120–210 mg were combined with a ^{229}Th – ^{233}U – ^{236}U tracer, digested, and purified via iron co-precipitation and ion exchange chromatography. Separate U and Th aliquots were analyzed using a Nu Plasma II-ES multi-collector ICP-MS equipped with a CETAC Aridus II desolvating nebulizer. ^{14}C and $^{230}\text{Th}/\text{U}$ ages were combined and all ages are presented on the ^{14}C timescale where 1950 CE (Common Era) = 0 ^{14}C yr BP. We assigned an age of -65 yr BP (for collection year of 2015) to the top of the actively growing stalagmite to construct an age model. The model used was a simple 2nd-order polynomial fit to the age depth data (Figure 3). Because our Asafora Cave stalagmite age model is based on both $^{230}\text{Th}/\text{U}$ and ^{14}C dates, we use “yr BP” instead of “Cal yr BP” in the text, recognizing that all ^{14}C dates have been calibrated. Thus, all ^{14}C dates (derived from fossils

and rock) reported in our Results and Discussion can be understood to have been calibrated unless otherwise indicated.

It is worth noting that ^{14}C age determinations are rarely used to develop age models for stalagmites because some, usually unknown, fraction of C in the samples is derived from the overlying bedrock carbonate, which is free of ^{14}C . For AF2, however, the uppermost ^{14}C age determination had greater than modern ^{14}C , suggesting that the Dead Carbon Fraction (DCF) of AF2 is close to zero and that the ^{14}C ages can be used without correction for a non-zero DCF. This interpretation is supported by the observation that AF2 was actively growing at the time of collection, and by the good agreement between

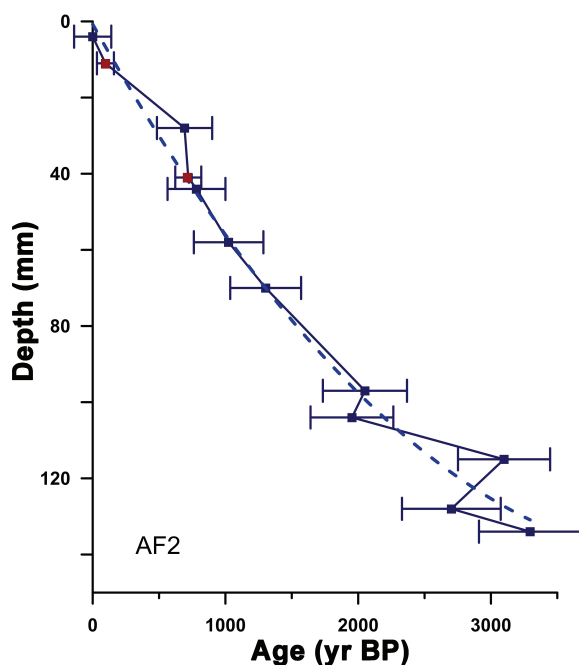


Figure 3. AF2 Age-depth data (based on $^{230}\text{Th}/\text{U}$ and calibrated ^{14}C determinations): This plot shows the $^{230}\text{Th}/\text{U}$ (red) and carbon age determinations (blue) with 2σ errors vs. depth for each sample.

Table 2. $^{230}\text{Th}/\text{U}$ age data for AF2 (Assafora Cave).

Z (distance in mm from top)	$^{238}\text{U} \pm (2\sigma)$ (ng/g) ^a	$^{232}\text{Th} \pm (2\sigma)$ (pg/g) ^a	$\delta^{234}\text{U} \pm (2\sigma)$ (per mil) ^b	$(^{230}\text{Th}/^{238}\text{U}) \pm (2\sigma)$	$^{230}\text{Th}/^{232}\text{Th} \pm (2\sigma)$	Age (yr) ± (2 σ)	$\delta^{234}\text{U}$ initial	Age (yr) ± (2 σ)	$\delta^{234}\text{U}$ initial	Age (yr) ± (2 σ)								
11	53	1	221	5	33	3	0	0	8	1	215	21	95	64	33	3	30	64
41	37	1	184	4	30	2	0.00881	0.00061	28	2	937	65	790	98	30	2	720	98

Notes:

^aReported errors for ^{238}U and ^{232}Th concentrations are estimated to be ± 1% due to uncertainties in spike concentration; analytical uncertainties are smaller.

^b $d^{234}\text{U} = [(^{234}\text{U}/^{238}\text{U}]_{\text{activity}} - 1] \times 1000$.

^c $[^{230}\text{Th}/^{238}\text{U}]_{\text{activity}} = 1 - e^{-t/^{230}\text{Th}} + (d^{234}\text{U}_{\text{measured}}/1000)[I_{230}/(I_{230} - I_{234})](1 - e^{-(t/^{230}\text{Th}) - t/^{234}\text{U}})$, where T is the age. "Uncorrected" indicates that no correction has been made for initial ^{230}Th .

^dAges are corrected for detrital ^{230}Th assuming an initial $^{230}\text{Th}/^{232}\text{Th}$ of $(4.4 \pm 2.2) \times 10^{-6}$.

^e $d^{234}\text{U}_{\text{initial}}$ corrected was calculated based on ^{230}Th age (T), i.e., $d^{234}\text{U}_{\text{initial}} = d^{234}\text{U}_{\text{measured}} X e^{t/^{234}\text{T}}$, and T is corrected age.

^fB.P. stands for "Before Present" where the "Present" is defined as the 1 January 1950 C.E.

calibrated ^{14}C ages and $^{230}\text{Th}/\text{U}$ ages for the upper part of the stalagmite.

Regional comparisons

Stable carbon and oxygen isotope data from AF2 were compared with published data for stalagmite AB2 from Anjohibe Cave, northwest Madagascar (Scroxton et al., 2017) (Figure 4). Sampling methods for AB2 are described in detail by Scroxton et al. (2017); 1069 subsamples were taken at intervals varying from 0.2 to 2 mm depending on the stalagmite's varying growth rate, resulting in the very high resolution of one sample every ~2 years. This allowed us to compare AF2 to AB2, both at high resolution.

Due to the influences of isotopic changes in the atmosphere, soil, and karst, it is important to recognize that $\delta^{18}\text{O}$ values cannot be directly compared for stalagmites from different regions (Fairchild, 2006). Dissimilar values will not necessarily reflect different rainfall amounts. Instead, when comparing oxygen isotopes, it is the shape and direction (but not magnitude or actual values) of change that are important. In contrast, $\delta^{13}\text{C}$ values can generally be directly compared and related to the dominance of different types of plant using different photosynthetic pathways (C_3 , CAM, and C_4) in the surrounding region. Pure C_3 habitats can produce carbon isotope values in speleothems between -6 to -14‰, while pure CAM or C_4 habitats can produce speleothem values of -6 to +2‰ (McDermott, 2004). Thus, the ratio of C_3 vs. CAM/ C_4 in the overlying vegetation is an important control on speleothem $\delta^{13}\text{C}$ values. However, smaller (<4‰) variations in $\delta^{13}\text{C}$ are likely due to changes in soil and root respiration rates, plant water use efficiency, and in-cave fractionation. They do not necessarily signify any change in the C_3 versus CAM/ C_4 mixture of the overlying vegetation (Wong & Breecker, 2015).

Determining the timing of megafaunal collapse

We reconstructed the timing of megafaunal collapse in the southwest (spiny thicket ecoregion) and northwest (dry deciduous forest ecoregion) separately by analyzing the radiocarbon records of extinct and extant animal bones from subfossil sites within the age range 3000 to 0 yr BP. Our total sample was 256 dates from the spiny thicket and 56 dates from the dry deciduous forest. We obtained published dates from the literature and present 30 previously unpublished dates for subfossils from the spiny thicket and five

from the dry deciduous forest (Appendix 1). Twenty-nine new specimens were prepared by us following Sparks & Crowley (2018). Collagen preservation was confirmed using sample yield, stable isotope data, and atomic C: N ratios, and the collagenous residue was radiocarbon-dated at the Center for Accelerator Mass Spectrometry, Lawrence Livermore National Laboratory. All ^{14}C dates were calibrated following the same methods described above, using the SHCal13 calibration curve in Calib 7.1 (Hogg et al., 2013; Stuiver et al., 2020). We present average calibrated dates ± 1 standard deviation (1σ) based on 2σ ranges (Appendix 1).

We followed Godfrey et al. (2019) in using odds ratio analysis (Bishop et al., 1975) to identify the timing of megafaunal collapse (i.e., the time of the greatest shift at subfossil sites from odds favoring the presence of extinct animals to odds favoring the presence of extant animals) for each ecoregion. Odds ratio analysis allows us to describe the trajectory of megafaunal decline, including the timing of most rapid change. We stress that this is not the same as the time of extinction, as populations of endangered species can persist for centuries (although in strongly reduced numbers) after they crash.

For each ecoregion, the maximum likelihood χ^2 values for cutpoints at 100-year intervals between

Table 3. Extinct and geographically restricted extant taxa from the spiny thicket and dry deciduous forest ecoregions that are represented in the radiocarbon database, with descriptions and sample size.

Class, Order	Genus	Common name; reconstructed habitat/diet; locomotion	No. of specimens	
			Spiny thicket	Dry deciduous forest
Mammalia, Primates	<i>Archaeolemur</i>	Monkey lemur; forest or woodland, fruit, leaves, seeds, structurally defended resources; semi-terrestrial quadruped.	17	10
	<i>Babakotia</i>	Sloth lemur; forest or woodland, arboreal folivore; arboreal, suspensory.	0	8
	<i>Daubentonia</i>	Giant aye-aye; forest or woodland, fruit, larvae, structurally defended resources; arboreal quadruped.	1	0
	<i>Hadropithecus</i>	Monkey lemur; succulent CAM foods; semi-terrestrial quadruped.	4	0
	<i>Megaladapis</i>	Koala lemur; forest or woodland; arboreal folivore; arboreal quadruped, slow vertical climber.	26	2
	<i>Mesopropithecus</i>	Sloth lemur; Forest or woodland; arboreal folivore; arboreal quadruped, slow climber, some suspension.	3	0
	<i>Pachylemur</i>	Giant ruffed lemur; forest or woodland; arboreal frugivore; arboreal quadruped.	15	0
	<i>Palaeopropithecus</i>	Sloth lemur; forest or woodland; arboreal folivore; arboreal slow climber, suspensory.	40	3
Mammalia, Carnivora	<i>Cryptoprocta</i>	Giant fossa; forest or woodland; faunivore; semi-terrestrial.	11	0
Mammalia, Rodentia	<i>Hypogeomys</i>	Malagasy giant jumping rat; frugivore, fruits and seeds; terrestrial.	3	0
	<i>Macrotarsomys</i> ¹	Petter's big-footed mouse; frugivore, feeding on fruits, berries, roots; terrestrial.	2	0
Mammalia, Artiodactyla	<i>Hippopotamus</i>	Pygmy hippopotamus; terrestrial herbivore; wetlands, forests, woodlands; semi-aquatic; facultative swimmer.	29	10
Aves, Anseriformes	<i>Alopochen</i>	Malagasy shelduck; lakes and swamps; seeds, leaves, grasses, plants; aquatic.	1	0
Aves, Cuculiformes	<i>Coua</i>	Giant couas; forest or woodland, feeding on insects and fruits; terrestrial, flightless.	1	0
Aves, Aepyornithiformes	<i>Aepyornis</i>	Elephant bird; terrestrial herbivore, C ₃ foods; terrestrial, flightless.	16	1
	<i>Mullerornis</i>	Elephant bird; terrestrial herbivore, C ₃ foods; terrestrial, flightless.	6	1
	<i>Vorombe</i>	Elephant bird; terrestrial herbivore, C ₃ foods; terrestrial, flightless.	2	0
Reptilia, Testudines	<i>Aldabrachelys</i>	Giant tortoise; terrestrial herbivore; terrestrial.	15	1
Reptilia, Crocodilia	<i>Voay</i>	Horned crocodile; faunivore; semi-aquatic; facultative swimmer.	1	0

¹ *Macrotarsomys petteri* is not extinct but its known range is severely reduced.

2000 yr BP and the year “0” (= 1950 CE) were calculated. Higher values for the maximum likelihood χ^2 signal a greater difference in the odds of finding extinct vs. extant taxa from before to after that cutpoint. We compared each trajectory of megafaunal decline to the associated time series plots for changes in speleothem $\delta^{13}\text{C}$ values. To better understand how climate-induced habitat change and human activities may have independently or synergistically affected the megafauna in the southwest, we also separately examined the distribution of extinct taxa across time at coastal and inland sites. In Table 3 we show the sample sizes for dated extinct genera (and extinct or very rare extant species within extant genera) from the spiny thicket and dry deciduous forest ecoregions, as well as some life history traits of these taxa.

Results

How did climate and vegetation change over the past several thousand years in the southwest?

Stalagmite AF2 from Asafora spans the period from ~3800 yr BP to present. The shapes of the stable oxygen ($\delta^{18}\text{O}$) and carbon ($\delta^{13}\text{C}$) isotope curves during this time span are similar (Figure 4) and their values are correlated ($r^2 = 0.47$; Figure 5). Such coupling is sometimes used as an indicator of kinetic isotopic effects on the isotopic records of a sample. However, because the cave from which the sample was collected has a single small entrance, is not well ventilated, and had nearly 100% humidity, we interpret the isotopic time series of AF2 to primarily reflect climate change. Carbon and oxygen isotopes may be correlated as a result of climate; decreases

in stalagmite drip rates resulting from a drier climate can, by themselves, lead to increased stalagmite $\delta^{13}\text{C}$ values.

The $\delta^{18}\text{O}$ curve suggests gradual aridification (with considerable fluctuation) beginning ~3300 years ago (Figure 4). The wettest interval was between ~3350 to ~3180 yr BP. A gradual increase in $\delta^{13}\text{C}$ values (and correlated $\delta^{18}\text{O}$ values) is observed from around 3350 to around 1680 yr BP. At the beginning of this period, the habitat was dominated by C_3 plants (with values of $-10\text{\textperthousand}$ to $-7\text{\textperthousand}$). The ensuing positive trend likely resulted from decreasing vegetation activity (i.e., decreasing soil and root respiration rates) during gradual drying, although the trend could also reflect a gradual increase in C_4 and/or CAM plants.

Between 1680 and 1560 yr BP, there was a sharp decrease in rainfall (i.e., increase in $\delta^{18}\text{O}$ values), initiating a prolonged dry period from ~1560 to 880 yr BP. Simultaneously, between ~1680 and 1550 yr BP, $\delta^{13}\text{C}$ values rose sharply. Over the next ~670 years, $\delta^{13}\text{C}$ values ranged from $-5\text{\textperthousand}$ to $+1.0\text{\textperthousand}$, peaking in the year 880 BP at $+1.5\text{\textperthousand}$. When the change in $\delta^{13}\text{C}$ values is combined with the temporal trend in $\delta^{18}\text{O}$ values, the data suggest that, during the span between 1560 and 880 yr BP, this part of southwestern coastal Madagascar experienced low rainfall and was consistently dominated by C_4 and/or CAM plants. The positive $\delta^{13}\text{C}$ values towards the end of this period are strong indicators of drought.

Between 880 and 860 yr BP, a second major isotopic change occurred in the AF2 stalagmite. Oxygen isotope values dropped rapidly (from $-3.4\text{\textperthousand}$ to $-6.7\text{\textperthousand}$) signaling an abrupt return to relatively

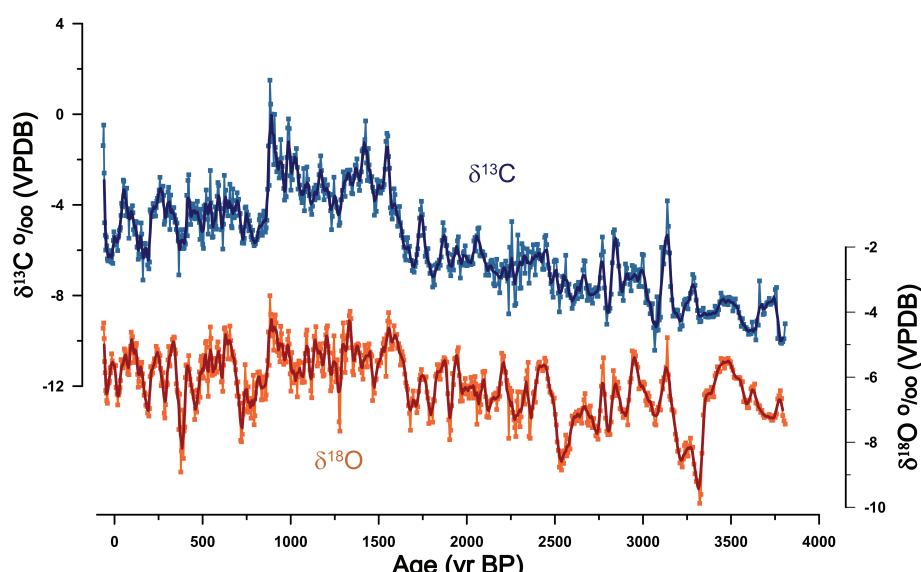


Figure 4. Time series of carbon (blue) and oxygen (orange) stable isotope ratios for stalagmite AF2 from Asafora Cave, southwest Madagascar. All ^{14}C dates are calibrated.

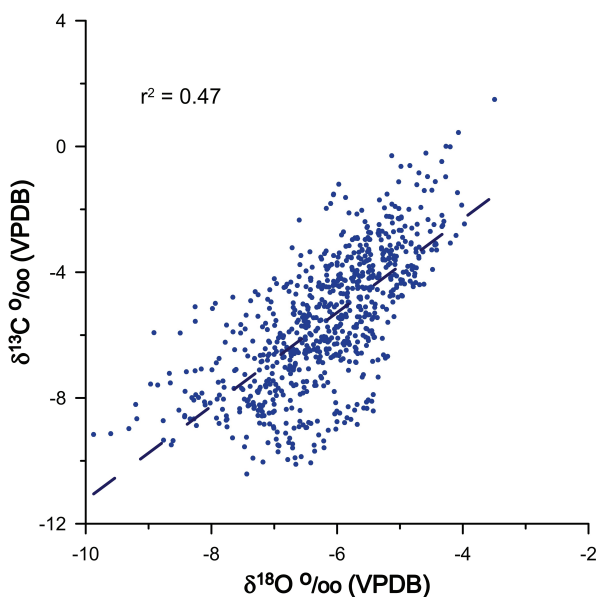


Figure 5. Scatter plot of stable carbon and oxygen isotope values for AF2, showing regression and variance explained.

wetter conditions. Simultaneously, carbon isotope values dropped from +1.5‰ to -5.2‰ signaling a return to a habitat with greater C_3 plant cover. From this point onward until very recently (post 860 yr BP but prior to 1950 CE), the climate was relatively moist, with some very wet intervals, but, overall, it was not as wet as the interval prior to the drought of the late first millennium. The $\delta^{13}\text{C}$ values stabilized around a mean of -4.7‰ (with a range of -7.3‰ to -2.4‰), indicating a vegetation with substantial C_3 plant cover and increased available moisture in this part of Madagascar.

Very recently (post-1950 CE), $\delta^{13}\text{C}$ values increased again by ~5‰ (from -6.2‰ to -1.4‰) in

tandem with a dramatic increase in oxygen isotope values, apparently reflecting severe drought. Indeed, episodic drought has been recorded over the past two decades in southern Madagascar (Bhalla, 2019) and during the late 20th century across the island (Ingram & Dawson, 2005).

Does the trajectory for climate change in the southwest match that of the northwest?

As revealed by the $\delta^{18}\text{O}$ trajectories for AF2 from Asafora Cave and AB2 from Anjohibe Cave, changes in rainfall over the past 1600 years in southwest and northwest Madagascar are not well correlated (Figure 6). Instead, they show rather opposing trends. During the last half of the first millennium CE, the northwest experienced its greatest rainfall of the past 1700 years, while the southwest experienced extended drought. The carbon isotope trajectories for AB2 and AF2 are also very different (Figure 7). In the southwest, as we have seen, changes in habitat over the past two millennia reflect changes in rainfall ($\delta^{18}\text{O}$ and $\delta^{13}\text{C}$ values are correlated). In the northwest, they do not.

Between the years 1540 and 1100 yr BP, the habitat around Anjohibe Cave was dominated by C_3 vegetation and there was little variation in $\delta^{13}\text{C}$ values (-4.7‰ to -8.5‰, averaging ~-7‰). Without any apparent change in $\delta^{18}\text{O}$ values, there was a sharp increase in $\delta^{13}\text{C}$ to a peak value (+3.7‰) between ~1100 and 960 yr BP. This abrupt decoupling of the AB2 $\delta^{13}\text{C}$ and $\delta^{18}\text{O}$ time series strongly suggests that habitat transformation in the northwest was anthropogenically driven. The $\delta^{13}\text{C}$ values remained

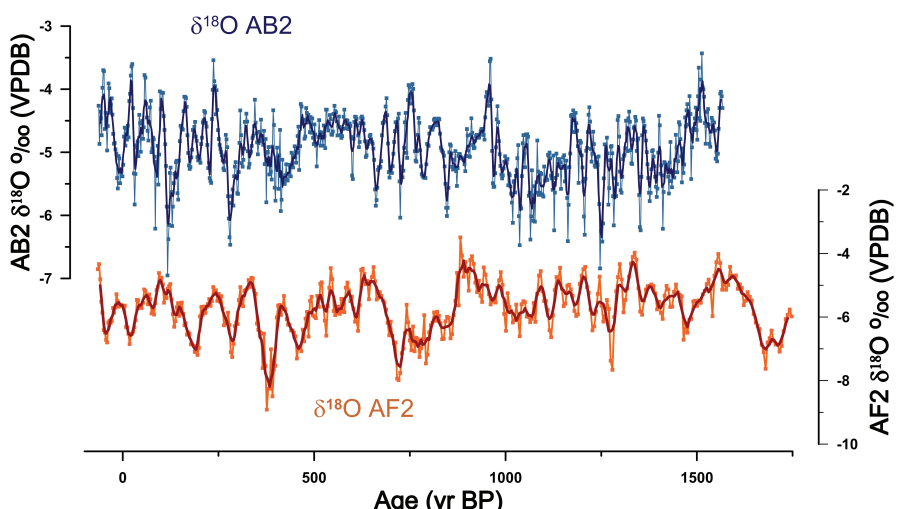


Figure 6. Comparison of time series of $\delta^{18}\text{O}$ values for stalagmites AB2 (blue, Anjohibe Cave, northwest Madagascar) and AF2 (orange, Asafora Cave, southwest Madagascar). All ^{14}C dates are calibrated.

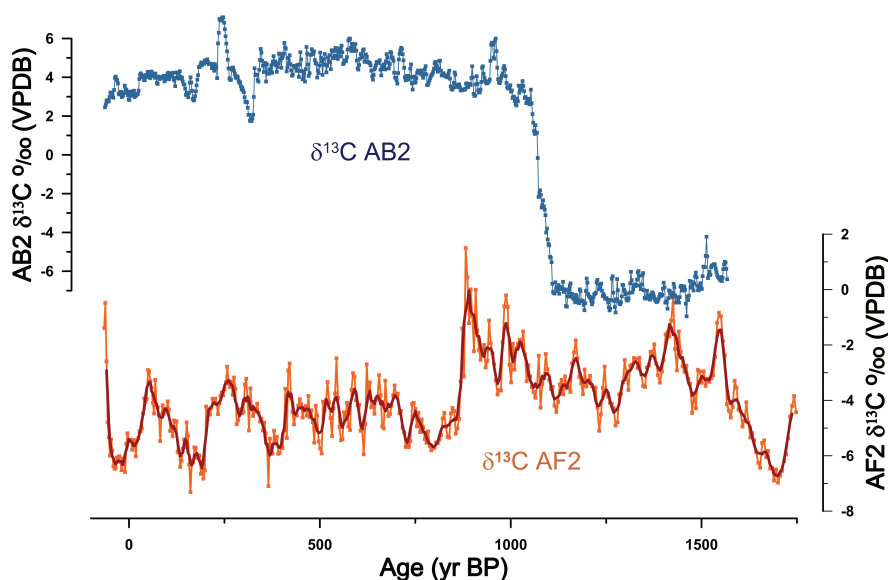


Figure 7. Comparison of time series of $\delta^{13}\text{C}$ values for stalagmites AB2 (blue, Anjohibe Cave, northwest Madagascar) and AF2 (orange, Asafora Cave, southwest Madagascar). All ^{14}C dates are calibrated.

highly elevated over the next millennium (Burns *et al.*, 2016), and likely reflect an open grassland such as that which persists in the region today. In summary, during the late Holocene, there were dramatic and diverging changes in $\delta^{13}\text{C}$ values in both the southwest and the northwest, with values increasing in the northwest and decreasing in the southwest. These data suggest an environmental response to different triggers with a strong anthropogenic influence in the northwest and climatic influences dominating in the southwest.

When did the megafauna crash?

The 2×2 tables used in our odds ratio analyses and the resulting maximum likelihood χ^2 values are presented in Table 4 and plotted in Figures 8a (for the spiny thicket) and 8c (for the dry deciduous forest). Figure 8 also displays the time series plots for changes in regional $\delta^{13}\text{C}$ values from stalagmites AF2 and AB2 (Figures 8b & 8d).

For the spiny thicket, there was little change in extinct-to-extant odds ratios prior to ~1700 yr BP (Figure 8a). Over a period of 500 years, from 1700 yr BP to 1200 yr BP, the megafauna declined slowly. This decline commenced as the $\delta^{18}\text{O}$ and $\delta^{13}\text{C}$ values began to shift, suggesting the onset of drought conditions and concomitant transformation to a habitat with increased representation of CAM and C_4 plants. The maximum likelihood χ^2 value representing the time of the greatest change in extinct-to-extant subfossil odds falls at 1100 yr BP. From 1100 yr BP onward, the χ^2 values fall rapidly with the

ongoing disappearance of megafaunal populations. Megafaunal stress appears to have begun with the shift to drought conditions, and to have accelerated after centuries of severe drought (Figures 8a & 8b).

The maximum likelihood χ^2 trajectory for the dry deciduous forest in the northwest is based on fewer data points (56 as opposed to 256 radiocarbon-dated individuals; Figure 8c), so it should be viewed with greater uncertainty than the corresponding trajectory from the spiny thicket. The smaller number of dated subfossil specimens may account for the lower χ^2 values. Nevertheless, the shape of the curve is informative, and there are some interesting similarities to, as well as differences from, that for the spiny thicket. For both ecoregions, there is a marked Late Holocene increase in the pace of megafaunal decline, but their relationships to variation in regional rainfall differ. In the southwest, aridification appears to have been an important stimulus. In the northwest, it was not (Burns *et al.*, 2016; Godfrey *et al.*, 2019).

Precipitous megafaunal decline began abruptly in the northwest in tandem with rapid vegetation transformation at 1100 yr BP and peaked at 1000 yr BP (Figures 8c & 8d). These indicators of megafaunal collapse in the dry deciduous forest occurred approximately 100 years later than the respective indicators in the spiny thicket ecoregion.

To better understand how climate-induced habitat change and human activities may have independently or synergistically affected the megafauna in the southwest, we examined the spatial and temporal distributions of extinct taxa in

Table 4. Odds ratio analysis: The pace of change in extinct-to-extant subfossil odds, quantified using the maximum likelihood χ^2 statistic for forty 2 x 2 tables (20 for the spiny thicket and 20 for the dry deciduous forest ecoregions). Age range for subfossil dates: 0 - 3000 yr BP. All ^{14}C dates are calibrated.

Before and after cutpoint (Cal yr BP)	Spiny thicket			Dry deciduous forest		
	Frequency extinct	Frequency extant	Maximum likelihood χ^2	Frequency extinct	Frequency extant	Maximum likelihood χ^2
<100	0	14	23.03	0	13	14.51
>100	162	80		21	22	
<200	0	25		0	15	17.28
>200	162	69	54.90	21	20	
<300	0	30	67.25	0	25	35.11
>300	162	64		21	10	
<400	0	33	74.92	0	29	45.49
>400	162	61		21	6	
<500	1	35	71.64	0	29	45.49
>500	161	59		21	6	
<600	2	37	70.92	0	29	45.49
>600	160	57		21	6	
<700	2	40	78.76	0	30	48.63
>700	160	54		21	5	
<800	3	48	95.50	0	30	48.63
>800	159	46		21	5	
<900	4	56	114.43	1	30	40.24
>900	158	38		20	5	
<1000	6	63	127.87	1	32	47.32
>1000	156	31		20	3	
<1100	10	81	182.57 (peak)	6	32	24.73
>1100	152	13		15	3	
<1200	31	84	130.36	8	33	21.84
>1200	131	10		13	2	
<1300	42	86	114.75	9	33	18.97
>1300	120	8		12	2	
<1400	53	89	107.94	10	33	16.29
>1400	109	5		11	2	
<1500	70	91	89.53	12	33	11.47
>1500	92	3		9	2	
<1600	76	91	80.21	13	33	9.31
>1600	86	3		8	2	
<1700	91	91	59.20	13	33	9.31
>1700	71	3		8	2	
<1800	95	91	54.08	13	33	9.31
>1800	67	3		8	2	
<1900	103	93	55.24	13	33	9.31
>1900	59	1		8	2	
<2000	108	93	49.09	14	33	7.31
>2000	54	1		7	2	

the spiny thicket before, during, and after the drought (Table 5). Most of the well-represented subfossil sites in this ecoregion are coastal, and consequently, inland sites are underrepresented in the radiocarbon database (Appendix 1). Nevertheless, it is instructive to examine them separately, as drought may have impacted coastal and inland sites differently (Crowley et al., 2017; Hixon et al., 2018).

Table 5 tracks extinct vertebrate species known to be present in the spiny thicket ecoregion prior to the drought; it shows whether they are known to have persisted in this region during and after the drought. Twelve of the 16 species known to be present in

the spiny thicket prior to the drought persisted into the drought, often well into the drought, after which the number drops precipitously to between three and five (Table 5). Terrestrial and semi-aquatic herbivores (such as hippopotamuses and elephant birds) were abundant in the southwest during the drought (Appendix 1). They appear to have increased in relative abundance as the relative abundance of large-bodied, arboreal primates declined. After the drought, there is scant evidence of large endemic vertebrate survival along the coast, but some species survived well into the last millennium at inland sites both in the spiny thicket (such as Ankilitelo; see

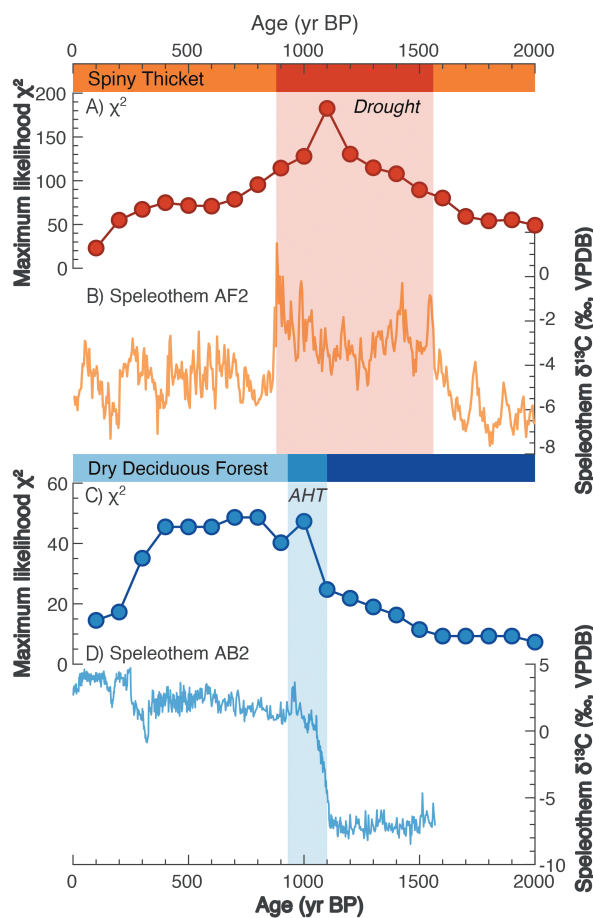


Figure 8. Comparisons of megafaunal decline trajectories (described by maximum likelihood χ^2 values) for the spiny thicket and dry deciduous forest ecoregions to the corresponding time series plots for changes $\delta^{13}\text{C}$ values for stalagmites AF2 (Asafora Cave) and AB2 (Anjohibe Cave). **A)** Megafaunal decline trajectory for the spiny thicket ecoregion; **B)** $\delta^{13}\text{C}$ time series for speleothem AF2; **C)** Megafaunal decline trajectory for the dry deciduous forest ecoregion; **D)** $\delta^{13}\text{C}$ time series for speleothem AB2. AHT = Anthropogenic Habitat Transformation. All ^{14}C dates are calibrated.

Simons et al., 1995; Muldoon et al., 2009; Muldoon & Goodman, 2010) and in the succulent woodlands (such as Tsirave). Inland sites may have remained hospitable to a wide variety of taxa, including forest-dwellers, longer than did coastal habitats (Table 5). While late dates confirm survival at Ankilitelo only for *Palaeopropithecus* and *Megaladapis*, bones of these animals were associated with those of other extinct primates (*Daubentonia robusta*, *Archaeolemur*, and *Pachylemur*) – taxa which Muldoon et al. (2009) argued may have also survived here until ~ 500 years ago.

Daubentonia robusta is known to have also survived at a coastal site in the extreme south, Beloha Anavoha, for at least a brief time after the drought ended. However, it is not known whether vertebrate species more dependent on freshwater habitats

Table 5. Presence/absence of radiocarbon-dated remains of extinct or broadly extirpated species at subfossil sites in the spiny thicket ecoregion (by temporal period and location, C = coastal, I = inland).

Taxon (order, genus, species)	Spiny thicket ecoregion		
	Pre-drought	Drought	Post-drought
Primates			
<i>Palaeopropithecus ingens</i>	+(C,I)	+(C,I)	+(I)
<i>Megaladapis edwardsi</i>	+(C)	+(C)	-
<i>Megaladapis madagascariensis</i>	+(C,I)	+(C,I)	+(I)
<i>Archaeolemur majori</i>	+(C,I)	+(C,I)	? (I)
<i>Pachylemur insignis</i>	+(C,I)	+(C,I)	? (I)
<i>Mesopropithecus globiceps</i>	+(C)	+(C)	-
<i>Hadropithecus stenognathus</i>	+(C)	-	-
Artiodactyla			
<i>Hippopotamus lemerlei</i>	+(C,I)	+(C,I)	-
Carnivora			
<i>Cryptoprocta spelea</i>	+(C,I)	-	-
Cuculiformes			
<i>Coua primaeva</i>	+(C)	-	-
Aepyornithiformes			
<i>Aepyornis</i> spp.	+(C,I)	+(C)	-
<i>Mullerornis modestus</i>	+(C)	+(C)	-
Rodentia			
<i>Hypogeomys australis</i>	+(C)	+(C)	-
<i>Macrotarsomys petteri</i>	+(C)	+(C)	-
Testudines			
<i>Aldabrachelys</i> sp.	+(C,I)	+(C,I)	+(C)
Crocodilia			
<i>Voay robustus</i>	+(C)	-	-
Total # of taxa	16	12	3-5

+: This taxon has specimens in the database with calibrated dates that fall in this period.

-: This taxon has no specimens in the database with calibrated dates that fall in this period.

?: This taxon occurs in apparent association with radiocarbon-dated specimens that fall in this period.

outlasted the drought in the southwest (Rasolonjatovo et al., 2021). One species, the Malagasy shelduck, *Alopochen sirabensis*, is known to have survived at Beloha Anavoha during the drought (1232 ± 177.5 yr BP; Goodman & Rakotozafy, 1997).

Discussion

The results reported here highlight, for the first time, strong evidence for regional variation in the impacts of climate vs. human activity on megafaunal extinction, and they raise new questions regarding their interactions. We presented here the precisely dated, high resolution records of hydroclimate and habitat change in the southwest needed to reconcile several contrasting hypotheses and better understand the complex regional processes behind Malagasy

megafaunal decline. Our data document drought conditions at Asafora Cave beginning ~1560 yr BP and lasting through the end of the first millennium and slightly beyond (until ~880 yr BP). This would appear to offer some support to the Aridification hypothesis, but that support is regionally limited.

It is worth noting that, despite finding overwhelming evidence against island-wide aridification, Crowley et al. (2017) found isotopic evidence for decreasing moisture at Andolonomby (on the southwest coast) between ~3000 yr BP and 1075 yr BP. Pollen from a sediment core retrieved at the same site (Virah-Sawmy et al., 2016) showed a sharp decline in *Pandanus* palms at 1574 yr BP that continued over the next several centuries. Between ~1600 and 700 yr BP, additional C₃ trees (*Antidesma*, *Dalbergia*, and *Uapaca*) and even some CAM plants (*Euphorbia*, and trees in the family Didiereaceae) declined or locally disappeared. Vallet-Coulomb et al. (2006) tracked changes in pollen diagrams and hydrological conditions at Lake Ihotry on the west coast 120 km north of Andolonomby. They found open water until ~2250 yr BP, a prolonged period of drying thereafter, and a shift to saline water conditions beginning around 1530 yr BP, when this region experienced an abrupt decline in palm pollen. The coincidence in the estimated timing of the onset of drought conditions at Asafora Cave (1560 yr BP), the abrupt decline in *Pandanus* (at 1574 yr BP) and subsequent loss of other C₃ trees at Andolonomby (Virah-Sawmy et al., 2016), as well as the onset (at ~1500 yr BP) of saline water conditions at Lake Ihotry (Vallet-Coulomb et al., 2006), cannot be accidental.

Our new data suggest that whereas the trajectories of megafaunal extinction differed in different ecoregions and whereas the detailed sequences of events were not the same across the island, megafaunal collapse occurred broadly within the same several hundred-year period. Drought coincided with initial megafaunal decline in the subarid southwest, and megafaunal population collapse accelerated between 1200 and 1000 yr BP, under prolonged drought conditions. In the northwest, megafaunal collapse began when the hydroclimate was wet at 1100 yr BP, and peaked at ~1000 yr BP. The overlap in the timing of megafaunal collapse in different parts of Madagascar clearly cannot be attributed to climate change. This was likely an important factor only in the southwest, the driest part of Madagascar.

The population dynamics of sub-viable and declining species can drive differences in the timing

of megafaunal population collapse versus extinction. At least some megafauna survived in the southwest not merely through the height of the drought but for centuries past that point. People were present in the region of Asafora Cave throughout the drought (Douglass et al., 2018; Godfrey et al., unpublished data). However, at the nearby Velondriake Marine Reserve, multiple archaeological sites document little evidence of human interaction with the megafauna during the drought; these people exploited marine resources (Douglass et al., 2018). Butchery of now-extinct species did occur in the region during the early part of the first millennium CE (MacPhee & Burney, 1991) but it intensified only after 1200 yr BP (Godfrey et al., unpublished data), in the middle of the drought.

The local human populations in the southwest (and in other parts of Madagascar) began growing exponentially by around the beginning of the last millennium CE (Pierron et al., 2017), at which time pastoralists introduced domesticated animals into the subarid southwest (Hixon et al., 2021). Hixon et al. (2021) show that this introduction occurred before the megafauna of the region had entirely disappeared.

We argue here that the story of the megafaunal population collapse in the southwest must include not merely the drought but also the post-drought actions of growing populations of pastoralists and of their livestock. In the southwest, as in the northwest, the introduction of cattle (and other domesticated animals) was the likely catalyst of the final demise of megafaunal species. All regions of Madagascar were affected by the expansion of the Indian Ocean trade network and the introduction of domesticated plants and animals, whether the climate was wet or dry, and whether megafaunal populations were already under stress caused by climate change or not. Across Madagascar, the megafauna were squeezed out of their preferred habitats by humans and their commensals. During and in the aftermath of severe drought, animals typically track their preferred resources, and for most species, such mobility decreases extinction risk. However, when humans and their commensals “invade” across habitats of different types, access to resources may be impeded. Preferred habitats may become highly fragmented or disappear entirely.

Madagascar’s northwest experienced wholesale transformation from woodlands to open grasslands. In the southwest, subarid habitats are naturally fire resistant, and humans rarely set fires to support their cattle and goats. The region has become, nevertheless, a haven for cattle, and there is

archaeological and genetic support for an increase in human populations in the southwest even prior to the introduction of the popular cattle fodder, *Opuntia monacantha* (or *raketa*), in 1769. This was likely particularly true after the climate became more mesic not long after the beginning of the last millennium. Prior to the introduction of *Opuntia*, cattle in the southwest relied on a variety of native “water-food” plants (Kaufmann & Tsirahamba, 2006; Kaufmann, 2008). This included grass species such as *Heteropogon contortus*, spiny succulent trees such as *Euphorbia stenoclada* (*samata*), other succulent *Euphorbia* species such as *E. tirucalli*, shade trees such as *Tamarindus indicus* and others. In the subarid climate of the southwest, cattle do not graze on open grasslands, but rather prefer wooded landscapes that offer shade as well as food. Grasses may be sparse in the southwest but they are nutritious (Kaufmann, 2008). Hixon et al. (2021) present isotopic support for the notion that, early in the last millennium, when domesticated bovids and ovicaprids were first introduced into the southwest, these animals browsed on a combination of C_3 shrubs and trees, CAM succulents, and C_4 grasses.

The evidence of intense aridification seen in the $\delta^{18}\text{O}$ and $\delta^{13}\text{C}$ values for stalagmite AF2 from Asafora around the time of megafaunal decline does not obviate an important role for humans in the extinction of megafauna in the southwest. Given the fact that wholesale burning of large areas is rare in this part of Madagascar, it is not surprising that decoupling of $\delta^{18}\text{O}$ and $\delta^{13}\text{C}$ values did not occur here. We do see some megafaunal evidence of increased habitat aridification on the west coast (especially at Andolonomby), but we also see evidence that regional aridification did not necessarily result in a change in dietary regime of species, such as elephant birds, prior to their extinction (Tovondrafale et al. 2014).

Conclusion

Our high-resolution analysis of stable carbon and oxygen isotope values in stalagmite AF2 provides a new detailed climate record and insight into the paleoclimate and paleoecology of southwestern Madagascar over the past 3000 years. We draw the following main conclusions from our research:

- Madagascar did not experience synchronous island-wide changes in hydroclimate over the past several thousand years. In fact, the hydroclimate of the southwest was largely (but not entirely) out of phase with that of the northwest. The driest

period (allowing for minor fluctuations) recorded by AF2 in the southwest occurred near the end of the first millennium CE and the beginning of the last millennium CE, while the last half of the first millennium recorded by stalagmite AB2 in the northwest was wet.

- The hydroclimate of the southwest was relatively wet between 3320 and 1560 yr BP but getting drier. Between 1560 and 880 yr BP, the hydroclimate of the southwest was dry. From that point onward until very recently, the last millennium was consistently wetter than the first millennium CE.
- The vegetation of the southwest was likely predominantly C_3 prior to the prolonged drought. However, during that drought, the percentage of CAM/ C_4 plants may have increased. At around 880 yr BP, in tandem with the recorded increase in rainfall amount, the vegetation may have transitioned once again (with a relative increase in C_3 plants).
- The maximum likelihood χ^2 trajectory clearly identifies the 200-year timespan when the megafaunal populations of the spiny thicket effectively crashed (i.e., from ~1200 to 1000 yr BP).
- Whereas there is strong evidence of human-induced habitat change in the northwest, habitat changes in the southwest were apparently triggered by changes in rainfall amount. There was no interval where marked decoupling of the carbon and oxygen isotope signals occurs.
- The coincidence of drought and megafaunal decline in the southwest does suggest that drought played a major role but does not obviate a secondary role for human activities, either coincident with or following the drought. The megafauna collapsed everywhere near the end of the 1st millennium despite regional differences in hydroclimate, suggesting that other factors (relating to human activities and probably the introduction of agropastoralism) contributed to island-wide megafaunal extinction.

Acknowledgments

This research was conducted under a collaborative accord between the University of Massachusetts Amherst (Department of Geosciences, Department of Anthropology) and Université d'Antananarivo, Madagascar (Bassins sédimentaires Evolution Conservation). We thank the Ministry of Higher Education and Research, Ministry of Mines and

Strategic Resources, Ministry of Communication and Culture, and Madagascar National Parks, for granting us permission to conduct field research in southwestern Madagascar and to collect fossils and stalagmites. We gratefully acknowledge the assistance of the people of the region of Tampolove near Asafora Cave, as well as colleagues at the University of Massachusetts Amherst Stable Isotope Laboratory and Department of Geosciences, the McGee Lab for Paleoclimate and Geochronology, MIT Department of Earth, Atmospheric and Planetary Sciences, and the Center for Accelerator Mass Spectrometry at the Lawrence Livermore National Laboratory. This project was supported by the National Science Foundation USA [AGS-1702891 to Stephen J Burns, BCS-1750598 to Laurie R Godfrey, BCS-1749676 to Brooke E Crowley, and AGS-1702691 to David McGee]. We thank our two anonymous reviewers for suggestions that substantially improved this article.

References

- Akers, P. D., Brook, G. A., Railsback, L. B., Liang, F., Iannone, G., Webster, J. W., Reeder, P. P., Cheng, H. & Lawrence Edwards, R. 2016.** An extended and higher-resolution record of climate and land use from stalagmite MC01 from Macal Chasm, Belize, revealing connections between major dry events, overall climate variability, and Maya sociopolitical changes. *Palaeogeography, Palaeoclimatology, Palaeoecology*, 459: 268-288.
- Alvard, M. S. 1993.** Testing the ecologically noble savage hypothesis—interspecific prey choice by Piro hunters of Amazonian Peru. *Human Ecology*, 21 (4): 355-387.
- Beaujard, P. 2019.** *The worlds of the Indian Ocean. Volume 1, From the fourth millennium BCE to the sixth century CE*. Cambridge University Press, Cambridge, UK.
- Bhalla, N. 2019.** Drought leaves 366,000 “one step away from famine” in Madagascar: U.N. Thomson Reuters Foundation (news report, 6 June 2019).
- Bishop, Y. M. M., Fienberg, S. E. & Holland, P. W. 1975.** Structural models for counted data. In *Discrete multivariate analysis: Theory and practice*, pp. 9-55. MIT Press, Cambridge, Massachusetts.
- Blench, R. 2010.** Evidence for the Austronesian voyages in the Indian Ocean. In *The global origins and development of seafaring*, eds. A. Anderson, J. H. Barrett & K. V. Boyle, pp. 239-248. McDonald Institute Monographs, Cambridge, UK.
- Burgess, N. D., D'Amico Hales, J., Underwood, E. C., Dinerstein, E., Itoua, I., Newman, K., Olson, D., Ricketts, T., Schipper, J. & Underwood, E. 2004.** *Terrestrial ecoregions of Africa and Madagascar: A conservation assessment*. Island Press, Washington, DC.
- Burney, D. A. 1993.** Late Holocene environmental change in arid southwestern Madagascar. *Quaternary Research*, 40: 98-106.
- Burney, D. A. 1999.** Rates, patterns, and processes of landscape transformation and extinction in Madagascar. In *Extinction near time*, ed. R. D. E. MacPhee, pp. 145-164. Kluwer Academic/Plenum Publishers, New York.
- Burney, D. A., Robinson, G. S. & Burney, L. P. 2003.** *Sporormiella* and the late Holocene extinction in Madagascar. *Proceedings of the National Academy of Sciences of the USA*, 100 (19): 10800-10805.
- Burney, D. A., Burney, L. P., Godfrey, L. R., Jungers, W. L., Goodman, S. M., Wright, H. T. & Jull, A. J. T. 2004.** A chronology for late prehistoric Madagascar. *Journal of Human Evolution*, 47: 25-63.
- Burns, S. J., Godfrey, L. R., Faina, P., McGee, D., Hardt, B., Ranivoharimanana, L. & Randrianasy, J. 2016.** Rapid human-induced landscape transformation in Madagascar at the end of the first millennium of the Common Era. *Quaternary Science Reviews*, 134: 92-99.
- Crowley, B. E. 2010.** A refined chronology of prehistoric Madagascar and the demise of the megafauna. *Quaternary Science Reviews*, 29: 2591-2603.
- Crowley, B. E. & Samonds, K. E. 2013.** Stable carbon isotope values confirm a recent increase in grasslands in northwestern Madagascar. *The Holocene*, 23: 1066-1073.
- Crowley, B. E., Godfrey, L. R., Bankoff, R. J., Perry, G. H., Culleton, B. J., Kennett, D. J., Sutherland, M. R., Samonds, K. E. & Burney, D. A. 2017.** Island-wide aridity did not trigger recent megafaunal extinctions in Madagascar. *Ecography*, 40: 901-912.
- Crowther, A., Lucas, L., Helm, R., Horton, M., Shipton, C., Wright, H. T., Walshaw, S., Pawlowicz, M., Radimilahy, C. & Douka, K. 2016.** Ancient crops provide first archaeological signature of the westward Austronesian expansion. *Proceedings of the National Academy of Sciences of the USA*, 113: 663.
- Dewar, R. E., Radimilahy, C. M., Wright, H. T., Jacobs, Z., Kelly, G. O. & Berna, F. 2013.** Stone tools and foraging in northern Madagascar challenge Holocene extinction models. *Proceedings of the National Academy of Sciences of the USA*, 110: 12583-12588.
- Donque, G. 1975.** *Contribution géographique à l'étude du climat de Madagascar*. Nouvelle Imprimerie des Arts Graphiques, Tananarive.
- Dorale, J. A., Edwards, R. L., Ito, E., & González, L. A. 1998.** Climate and vegetation history of the midcontinent from 75 to 25 ka: A speleothem record from Crevice Cave, Missouri, USA. *Science*, 282 (5395): 1871-1874.
- Douglass, K., Antonites, A. R., Quintana Morales, E. M., Grealy, A., Bunce, M., Bruwer, C. & Gough, C. 2018.** Multi-analytical approach to zooarchaeological assemblages elucidates Late Holocene coastal lifeways in southwest Madagascar. *Quaternary International*, 471: 111-131.

- Douglass, K., Hixon, S., Wright, H. T., Godfrey, L. R., Crowley, B. E., Manjakahery, B., Rasolondrainy, T., Crossland, Z. & Radimilahy, C.** 2019. A critical review of radiocarbon dates clarifies the human settlement of Madagascar. *Quaternary Science Review*, 221: 105878.
- Fairchild, I. J., Smith, C. L., Baker, A., Fuller, L., Spölt, C., Mattey, D., McDermott, F. & E. I. M. F.** 2006. Modification and preservation of environmental signals in speleothems. *Earth-Science Reviews*, 75: 105-153.
- Godfrey, L. R., Scroxton, N., Crowley, B. E., Burns, S. J., Sutherland, M. R., Pérez, V. R., Faina, P., McGee, D. & Ranivocharimanana, L.** 2019. A new interpretation of Madagascar's megafaunal decline: The subsistence shift hypothesis. *Journal of Human Evolution*, 130: 126-140.
- Gommery, D., Ramanivosa, B., Faure, M., Guerin, C., Kerloc'h, P., Sénégas, F. & Randrianantenaina, H.** 2011. Les plus anciennes traces d'activités anthropiques de Madagascar sur des ossements d'hippopotames subfossiles d'Anjohibe. *Comptes Rendus Palevol*, 10: 271-278.
- Goodman, S. M. & Benstead, J. P.** 2005. Updated estimates of biotic diversity and endemism for Madagascar. *Oryx*, 39 (1): 73-77.
- Goodman, S. M. & Rakotozafy, L. M. A.** 1997. Subfossil birds from coastal locations in western and southwestern Madagascar: A paleoenvironmental reconstruction. In *Natural change and human impact in Madagascar*, eds. S. M. Goodman & B. D. Patterson, pp. 257-279. Smithsonian Institution Press, Washington, DC.
- Goodman, S. M., Raherilalao, M. J. & Wohlhauser, S. (eds.).** 2018. *The terrestrial protected areas of Madagascar: Their history, description, and biota. Volume III: Western and Southwestern Madagascar – Synthesis*. Association Vahatra, Antananarivo.
- Griffiths, J. F. & Ranaivoson, R.** 1972. *Climates of Africa*. Elsevier, Amsterdam.
- Hansford, J., Wright, P. C., Rasoamaramanana, A., Pérez, V. R., Godfrey, L. R., Erickson, D., Thompson, T. & Turvey, S. T.** 2018. Early Holocene human presence in Madagascar evidenced by exploitation of avian megafauna. *Science Advances*, 4 (9): eaat6925.
- Hixon, S. W., Elliot Smith, E. A., Crowley, B. E., Perry, G. H., Randrianasy, J., Ranaivoarisoa, J. F., Kennett, D. J. & Newsome, S. D.** 2018. Nitrogen isotope ($\delta^{15}\text{N}$) patterns for amino acids in lemur bones are inconsistent with aridity driving megafaunal extinction in southwestern Madagascar. *Journal of Quaternary Science*, 33: 958-968.
- Hixon, S. W., Douglass, K. G., Crowley, B. E., Rakotozafy, L. M. A., Clark, G., Anderson, A., Haberle, S., Ranaivoarisoa, J. F., Buckley, M., Fidiarisoa, S., Mbola, B. & Kennett, D. J.** 2021. Late Holocene spread of pastoralism coincides with endemic megafaunal extinction in Madagascar. *Proceedings of the Royal Society B*, 288: 2021.1204.
- Hogg, A. G., Hua, Q., Blackwell, P. G., Niu, M., Buck, C. E., Guilderson, T. P., Heaton, T. J., Palmer, J. G., Reimer, P. J., Reimer, R. W., Turney, S. M. & Zimmerman, S.**
- R. H.** 2013. SHCAL13 Southern hemisphere calibration, 0-50.000 years Cal BP. *Radiocarbon*, 55: 1889-1903.
- Ingram, J. C. & Dawson, T. P.** 2005. Climate change impacts and vegetation response on the island of Madagascar. *Philosophical Transactions of the Royal Society A*, 363: 55-59.
- Kaufmann, J. C.** 2008. The non-modern constitution of famines in Madagascar's spiny forests: "Water-food" plants, cattle and Mahafale landscape praxis. *Environmental Sciences*, 5 (2): 73-89.
- Kaufmann, J. C. & Tsirahamba, S.** 2006. Forests and thorns: Conditions of change affecting Mahafale pastoralists in southwestern Madagascar. *Conservation Society*, 4: 231-261.
- Koch, P. L. & Barnosky, A. D.** 2006. Late Quaternary extinctions: State of the debate. *Annual Review of Ecology Evolution Systematics*, 37: 215-250.
- Lachniet, M. S.** 2009. Climatic and environmental controls on speleothem oxygen-isotope values. *Quaternary Science Reviews*, 28: 412-432.
- MacPhee, R. D. E. & Burney, D. A.** 1991. Dating of modified femora of extinct dwarf hippopotamus from southern Madagascar: implications for constraining human colonization and vertebrate extinction events. *Journal of Archaeological Science*, 18: 695-706.
- Mahé, J. & Sourdat, M.** 1972. Sur l'extinction des vertébrés subfossiles et l'aridification du climat dans le Sud-Ouest de Madagascar. *Bulletin de la Société Géologique de France*, 14: 295-309.
- McDermott, F.** 2004. Paleo-climate reconstruction from stable isotope variations in speleothems: A review. *Quaternary Science Reviews*, 23: 901-918.
- Muldoon, K. M., De Blieux, D. D., Simons, E. L. & Chatrath, P. S.** 2009. The subfossil occurrence and paleoecological significance of small mammals at Ankilitelo Cave, southwestern Madagascar. *Journal of Mammalogy*, 90 (5): 1111-1131.
- Muldoon, K. M. & Goodman, S. M.** 2010. Ecological biogeography of Malagasy non-volant mammals: Community structure is correlated with habitat. *Journal of Biogeography*, 37: 1144-1159.
- Pérez, V. R., Godfrey, L. R., Nowak-Kemp, M., Burney, D. A., Ratsimbazafy, J. & Vasey, N.** 2005. Evidence of early butchery of giant lemurs in Madagascar. *Journal of Human Evolution*, 49: 722-742.
- Pierron, D., Heiske, M., Razafindrazaka, H., Rakoto, I., Rabetokotany, N., Ravololomanga, B., Rakotozafy, L. M.-A., Rakotomalala, M. M., Razafiarivony, M., Rasoarifetra, B., Raharijesy, M. A., Razafindralambo, L., Ramlisonina, Fanony, F., Lejamble, S., Thomas, O., Abdallah, A. M., Rocher, C., Arachiche, A., Tonaso, L., Pereda-Ioth, V., Schiavinato, S., Brucato, N., Ricaut, F.-X., Kusuma, P., Sudoyo, H., Ni, S., Boland, A., Deleuze, J.-F., Beaujard, P., Grange, P., Adelaar, S., Stoneking, M., Rakotoarisoa, J.-A., Radimilahy, C. & Letellier, T.** 2017. Genomic landscape of human diversity across Madagascar. *Proceedings of the National Academy of Sciences of the USA*, 114 (32): E6498-E6506.

- Railsback, L. B., Dupont, L. A., Liang, F., Brook, G. A., Burney, D. A., Cheng, H. & Edwards, R. L. 2020.** Relationships between climate change, human environmental impact, and megafaunal extinction inferred from a 4000-year multi-proxy record from a stalagmite from northwestern Madagascar. *Quaternary Sciences Reviews*, 234: 106244.
- Rasolonjatovo, H. A. M., Muldoon, K. M., Ranivoharimanana, L., Rakotoarijaona, M. & Goodman, S. M. 2021.** Subfossil birds from a submerged cave in southwestern Madagascar. *Malagasy Nature*, 15: 128-140.
- Razanatsoa, E. 2019.** Impact of human land-use and rainfall variability in tropical dry forests of southwest Madagascar during the late Holocene. Doctoral Dissertation, Department of Biological Sciences, University of Cape Town, South Africa.
- Robinson, J. G. & Bennett, E. L. 2000.** Carrying capacity limits to sustainable hunting in tropical forests. In *Hunting for sustainability in tropical forests*, eds. J. G. Robinson & E. L. Bennett, pp. 13-30. Columbia University Press, New York.
- Sauther, M. L., Bertolini, F., Dollar, L. J., Pomerantz, J., Alves, P. C., Gandolfi, B., Kurushima, J. D., Mattucci, F., Randi, E., Rothschild, M. F., Cuozzo, F. P., Larsen, R. S., Moresco, A., Lyons, L. A. & Youssouf Jacky, I. A. 2020.** Taxonomic identification of Madagascar's free-ranging "forest cats". *Conservation Genetics*, 21: 443-451.
- Scroxton, N. 2014.** Late Pleistocene climate and environment from speleothems on Flores, Indonesia: Vegetation, volcanoes and *Homo floresiensis*. Ph.D. thesis, The Australian National University, Canberra.
- Scroxton, N., Burns, S. J., McGee, D., Hardt, B., Godfrey, L. R., Ranivoharimanana, L. & Faina, P. 2017.** Hemispherically in-phase precipitation variability over the last 1700 years in a Madagascar speleothem record. *Quaternary Science Reviews*, 164: 25-36.
- Scroxton, N., Burns, S. J., McGee, D., Hardt, B., Godfrey, L. R., Ranivoharimanana, L. & Faina, P. 2019.** Competing temperature and atmospheric circulation effects on southwest Madagascan rainfall during the last deglaciation. *Paleoceanography and Paleoclimatology*, 34: 275-28.
- Simons, E. L., Burney, D. A., Chatrath, P. S., Godfrey, L. R., Jungers, W. L. & Rakotosaminanana, B. 1995.** AMS ^{14}C dates for extinct lemurs from caves in the Ankarana massif, northern Madagascar. *Quaternary Research*, 43: 249-254.
- Sparks, J. M. & Crowley, B. E. 2018.** Where did people forage in prehistoric Trinidad? Testing the utility of a multi-isotope approach for tracking the origins of terrestrial prey. *Journal of Archaeological Science Reports*, 19: 968-978.
- Stuiver, M., Reimer, P. J. & Reimer, R. W. 2020.** CALIB 7.1 [WWW program] at <http://calib.org>, accessed 2020-6-26.
- Tovondrafaile, T., Razakamanana, T., Hiroko, K. & Rasoamiaramanana, A. 2014.** Paleoecological analysis of elephant bird (*Aepyornithidae*) remains from the Late Pleistocene and Holocene formations of southern Madagascar. *Malagasy Nature*, 8: 1-13.
- Vallet-Coulob, C., Gasse, F., Robinson, L., Ferry, L., Van Campo, E. & Chalié, F. 2006.** Hydrological modeling of tropical closed Lake Ihoroy (SW Madagascar): Sensitivity analysis and implications for paleohydrological reconstructions over the past 4000 years. *Journal of Hydrology*, 331: 257-271.
- Virah-Sawmy, M., Willis, K. J. & Gillson, L. 2010.** Evidence for drought and forest declines during the recent megafaunal extinctions in Madagascar. *Journal of Biogeography*, 37: 506-519.
- Virah-Sawmy, M., Gillson, L., Gardner, C. J., Anderson, A., Clark, G. & Haberle, S. 2016.** A landscape vulnerability framework for identifying integrated conservation and adaptation pathways to climate change: The case of Madagascar's spiny forest. *Landscape Ecology*, 31: 637-654.
- Voarintsoa, N. R. G., Wang, L., Railsback, L. B., Brook, G. A., Liang, F., Cheng, H. & Edwards, R. L. 2017.** Multiple proxy analyses of a U/Th dated stalagmite to reconstruct paleoenvironmental changes in northwestern Madagascar between 370 CE and 1300 CE. *Paleogeography Paleoclimatology, Paleoecology*, 469: 138-155.
- Wang, L., Brook, G. A., Burney, D. A., Voarintsoa, N. R. G., Liang, F., Cheng, H. & Edwards, R. L. 2019.** The African Humid Period, rapid climate change events, the timing of human colonization, and megafaunal extinctions in Madagascar during the Holocene: Evidence from a 2 m Anjohibe Cave stalagmite. *Quaternary Sciences Reviews*, 210: 136-153.
- Winterhalder, B. 2001.** The behavioural ecology of hunter-gatherers. In *Hunter-gatherers: An interdisciplinary perspective*, eds. C. Panter-Brick, R. H. Layton & P. Rowley-Conwy, pp. 12-38. Cambridge University Press, Cambridge, UK.
- Wong, C. I. & Breecker, D. O. 2015.** Advancements in the use of speleothems as climate archives. *Quaternary Science Reviews*, 127: 1-18.
- Wright, H. T., Vérin, P., Ramilisonina, Burney, D., Burney, L. P. & Matsumoto, K. 1996.** The evolution of settlement systems in the Bay of Boeny and the Mahavavy river valley, north-western Madagascar. *Azania: Archeological Research in Africa*, 31: 37-73.

Appendix 1. New dates for subfossils (extinct and extant) from sites in the spiny thicket and dry deciduous forest ecoregions.¹

Ecoregion	Site name	Coastal or inland	Genus and species	Extinct (0)/ Extant (1)	Specimen #	^{14}C Age BP $\pm 1\sigma$	Mean Cal yr BP $\pm 1\sigma$	Lab #
Spiny thicket	Andrahomana	Coastal	<i>Microcebus</i> sp.	1	UMASS uncatalogued (#1158)	240 \pm 30	227.5 \pm 82.5	CAMS 147331
Spiny thicket	Andrahomana	Coastal	<i>Microcebus</i> sp.	1	UMASS uncatalogued (#207)	485 \pm 25	500 \pm 30	CAMS 147180
Spiny thicket	Andrahomana	Coastal	<i>Microcebus</i> sp.	1	UMASS uncatalogued (#237b)	430 \pm 25	417.5 \pm 87.5	CAMS 147118
Spiny thicket	Andrahomana	Coastal	<i>Microcebus</i> sp.	1	UMASS uncatalogued (#224)	345 \pm 25	377.5 \pm 72.5	CAMS 147106
Spiny thicket	Andrahomana	Coastal	<i>Microcebus</i> sp.	1	UMASS uncatalogued (#417)	300 \pm 25	360 \pm 80	CAMS 147328
Spiny thicket	Antsirafaly	Coastal	<i>Megaladapis edwardsi</i>	0	UA 10699	1550 \pm 20	1382.5 \pm 42.5	UCI/AMS 167900
Spiny thicket	Andrananovy	Coastal	<i>Macronycteris cf. commersoni</i>	1	UAP-01.158-a	135 \pm 20	127.5 \pm 127.5	CAMS 150527
Spiny thicket	Andrananovy	Coastal	Unidentified snake	1	UAP-01.158-r	160 \pm 25	137.5 \pm 137.5	CAMS 148385
Spiny thicket	Vintany	Coastal	<i>Macronycteris cf. commersoni</i>	1	UABEC 0901	1950 \pm 30	1855 \pm 70	CAMS 182449
Spiny thicket	Vintany	Coastal	<i>Pachylemur insignis</i>	0	UABEC 0821	2830 \pm 130	2982.5 \pm 282.5	CAMS 182448
Spiny thicket	Vintany	Coastal	<i>Pachylemur insignis</i>	0	UABEC 0824	2155 \pm 30	2080 \pm 75	CAMS 182344
Spiny thicket	Antsirafaly	Coastal	<i>Mulleromys modestus</i>	0	UABEC 1372	1945 \pm 25	1860 \pm 60	CAMS 183974
Spiny thicket	Antsirafaly	Coastal	<i>Mulleromys modestus</i>	0	UABEC 1382	1465 \pm 25	1325 \pm 35	CAMS 183969
Spiny thicket	Soalara	Coastal	<i>Mulleromys modestus</i>	0	UABEC 1476A	1305 \pm 25	1180 \pm 90	CAMS 183967
Spiny thicket	Soalara	Coastal	<i>Mulleromys modestus</i>	0	UABEC 1476B	1270 \pm 25	1125 \pm 60	CAMS 183966
Spiny thicket	Soalara	Coastal	<i>Mulleromys modestus</i>	0	UABEC 1385	1595 \pm 25	1447.5 \pm 72.5	CAMS 183965
Spiny thicket	Antsirafaly	Coastal	<i>Vorombe titan</i>	0	UABEC 1434	1540 \pm 25	1367.5 \pm 52.5	CAMS 183968
Spiny thicket	Antsirafaly	Coastal	<i>Vorombe titan</i>	0	UABEC 1414	1675 \pm 25	1517.5 \pm 67.5	CAMS 183949
Spiny thicket	Antsirafaly	Coastal	<i>Hippopotamus lemerlei</i>	0	UABEC 1378	1580 \pm 25	1440 \pm 75	CAMS 183970
Spiny thicket	Antsirafaly	Coastal	<i>Hippopotamus lemerlei</i>	0	UABEC 1391	1940 \pm 25	1825 \pm 80	CAMS 183973
Spiny thicket	Antsirafaly	Coastal	<i>Hippopotamus lemerlei</i>	0	UABEC 1377	1620 \pm 25	1470 \pm 65	CAMS 183975
Spiny thicket	Antsirafaly	Coastal	<i>Archaeolemur majori</i>	0	UABEC 1349	1310 \pm 25	1185 \pm 90	CAMS 183972
Spiny thicket	Antsirafaly	Coastal	<i>Megaladapis edwardsi</i>	0	UABEC 1371	1660 \pm 25	1497.5 \pm 72.5	CAMS 183950
Spiny thicket	Vintany Cave	Coastal	<i>Microcebus griseorufus</i>	1	UABEC 0744	2325 \pm 45	2250 \pm 110	CAMS 185375
Spiny thicket	Mitoho Cave	Coastal	<i>Macronycteris cf. commersoni</i>	1	UABEC 1287a	0	0	CAMS 183951
Spiny thicket	Mitoho Cave	Coastal	<i>Macronycteris cf. commersoni</i>	1	UABEC 1287b	1525 \pm 25	1360 \pm 50	CAMS 183971
Spiny thicket	Soarano Cave	Coastal	<i>Voay robustus</i>	0	UABEC 1358	2340 \pm 30	2270 \pm 85	CAMS 183952
Spiny thicket	West Mikoboka Plateau Cave #8	Inland	<i>Eliurus</i> sp.	1	DPC 24129b	25 \pm 25	25	CAMS 147330
Spiny thicket	West Mikoboka Plateau Cave #12	Inland	<i>Eulemur</i> sp.	1	DPC 24140	0	0	CAMS 147112
Spiny thicket	Anjohibe	Inland	<i>Canis familiaris</i>	1	DPC 24128	0	0	CAMS 147307
Dry deciduous forest	Anjohikely	Inland	<i>Macronycteris cf. commersoni</i>	1	Uncatalogued	200 \pm 25	180 \pm 110	CAMS 147110
Dry deciduous forest	Beanka	Inland	<i>Lemur catta</i>	1	UAP-03.378-1	0	0	CAMS 148396
Dry deciduous forest	Beanka	Inland	<i>Eulemur cf. rufus</i>	1	UA uncatalogued	1105 \pm 25	995 \pm 60	CAMS 178785
Dry deciduous forest	Beanka	Inland	<i>Propithecus cf. deckenii</i>	1	UA uncatalogued	1130 \pm 25	987.5 \pm 62.5	CAMS 178786

¹ All specimens with >modern ^{14}C concentration were given an assigned age of 0 yr BP. UA 10699 was prepared at the Pennsylvania State University's Human Paleoecology and Isotope Geochemistry Lab and dated at the Keck-Carbon Cycle AMS facility, University of California, Irvine. For all other specimens, see Methods.